DEVELOPMENT OF THE BEST-ESTIMATE SYSTEM TRANSIENT ANALYSIS CODE, SSC-K, FOR POOL-TYPE LIQUID METAL REACTORS

Kyung-Doo Kim, Yong-Min Kwon, Dohee Hahn, Won-Pyo Chang and Soo-Dong Suk
Korea Atomic Energy Research Institution, P.O. Box 105, Yusung, 305-606, Taejon, Korea

ABSTRACT
The SSC-K code is a best-estimate system analysis code for the analyses of steady-state conditions and transients in pool type liquid metal reactors. It is developed on the basis of the SSC-L originally developed at BNL to analyze loop-type liquid metal reactor transients. Because of operational characteristic difference between the pool and loop designs, the major modifications of SSC-L have been made for the safety analysis of KALIMER. The code uses a one-dimensional representation of single-phase flow that solves conservation equations for mass, energy, and momentum for liquid phase. The paper will focus on the modeling descriptions and logical verification results to illustrate the simulation capabilities for pool-type liquid metal reactor transients. The paper also describes some of capabilities on a post-processor developed to effectively analyze SSC-K simulation results.

1. INTRODUCTION

The Supper System Code of KAERI (SSC-K) is a best-estimate system code for analyzing an variety of off-normal or accidents in KALIMER [1]. It is developed at Korea Atomic Energy Research Inititute (KAERI) on the basis of SSC-L originally developed at BNL to analyze loop-type LMR transients [2]. Because the dynamic response of the primary coolant in a pool-type LMR, particularly the hot pool concept like KALIMER, can be quite different from that in the loop-type LMR, the major modifications of SSC-L have been made for the safety analysis of KALIMER.

The major difference between KALIMER and general loop type LMRs exists in the primary heat transport system as shown in Fig. 1. In KALIMER, all of the essential components composing the primary heat transport system are located within the reactor vessel. They include the reactor, four EM

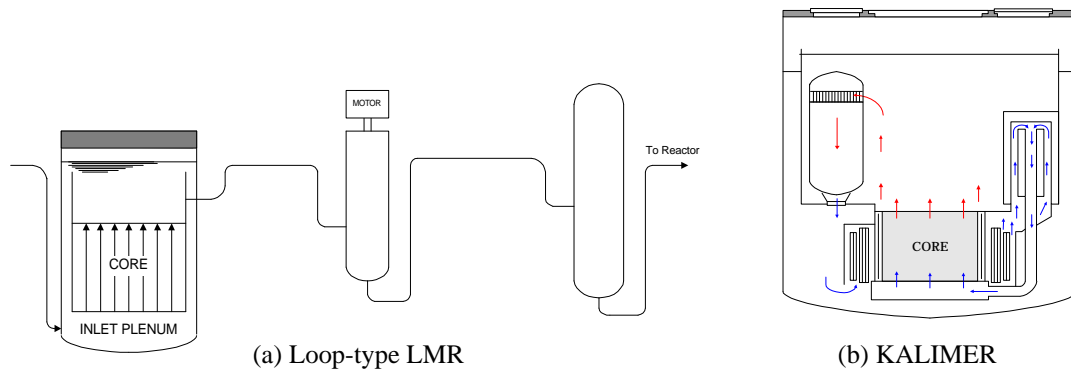(a) Loop-type LMR   (b) KALIMER

Fig. 1: Primary System Schematics

pumps, the primary side of four intermediate heat exchangers, sodium pools, cover gas blanket, and associated pipings. This is contrast to the loop type LMRs, in which all the primary components are connected via piping to form loops external to the reactor vessel. KALIMER has only one cover gas space. This eliminates the need for the separate cover gas systems over liquid level in pump tanks and

upper plenum. The IHX outlet is directly connected to cold pool instead of the piping into pump suction which is a typical configuration in loop type LMRs. Since the sodium in the hot pool is separated from the cold pool by insulated barrier in KALIMER, the liquid level in the hot pool is different from that in the cold pool mainly due to hydraulic losses and pump suction heads occuring during flow through the circulation pathes. In some accident conditions the liquid in the hot pool is flooded into the cold pool and forms a natural circulation flow path. During the loss of heat sink transients, this will provide as a major heat removal mechanism with the passive decay heat removel system. Since the pipes in the primary system exist only between the pump discharge and the core inlet plenum and are submerged in the cold pool, a pipe rupture accident becomes less severe because of a constant back pressure exerted against the coolant flow from break.

2. GENERAL MODELING DESCRIPTION

Fig. 2 shows a schematic of SSC-K Modeling for KALIMER. As it may be noticed, there is a pipe after IHX which do not exist in KALIMER. This pipe is included to minimize the modification of the loop type version of the SSC-K. This pipe is used to make the elevation of IHX exit the same as the elevation of pump inlet. The pump surge tank model in the loop-type version of SSC is used as a basis of the cold pool model in KALIMER. The pump surge tank in the loop-type LMR has similar characteristics with the cold pool in the pool-type LMR in many aspects. Both components include two distinct regions. The sodium is present in lower region, while the upper part is filled with non-condensable gas on the top of the sodium. The sodium levels in both components are changing with mass balance between the IHX exit flow and the pump inlet flow. However, some differences exist between two components. First, cover gas in the pump surge tank is separated by the cover gas in the vessel while the cover gas in the cold pool is in common with the cover gas above the hot pool. Second, the enthalpy in the pump surge tank is assumed to be the same as the enthalpy of the IHX exit flow. This is a reasonable assumption for the pump surge tank because of its small volume. However, it is not true in the cold pool. Therefore, energy equation is added in the cold pool model to account the energy stored in the sodium. Thus it is assumed that the entire pump inlet flow is from the cold pool and no direct flow from the IHX exit. As seen in Fig. 2, a few variables are newly defined to model the cold pool and their descriptions are as follows:

Fig. 2: Schematic of SSC-K Modeling for KALIMER

V6BPMP: Volume below pump inlet
Z6IHXP: Elevation changes from pump suction to IHX exit
A6IHXP: Average flow area from pumps suction to IHX exit
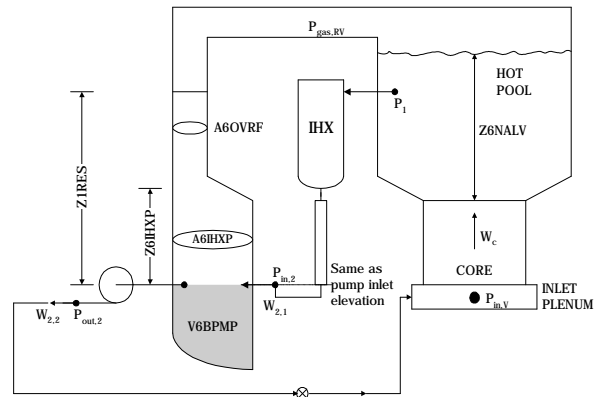A6OVRF: Average flow area for overflow path

2.1 Flow Equations

In the loop-type designs, direct pipe connections permit basically the use a single momentum equation to characterize the coolant behaviors in the primary loop, except in a transient initiated by pipe rupture. In KALIMER, both the hot and cold pools have free surfaces and there is direct mixing of the coolant with these open pools prior to entering the next component. Therefore, at least two different flows would have to be modeled to characterize the coolant dynamics of the primary system. Since the primary system of KALIMER has same number of pumps and IHXs, the current version of

the SSK-K has developed with constraint that the number of pumps has to be the same as the number of IHXs.

2.1.1 Intact System

The flow from the pump to core inlet plenum would respond to the pump head and losses in that circuit. For an intact system, volume-averaged momentum equations for pump outlet flow can be written as follows:

$$\frac{dW_p(k)}{dt} \sum_p \frac{L(k)}{A(k)} = P_{Po}(k) - P_{Rin} - \sum_p \Delta P_{f,g}(k), \qquad k = 1, \cdots, N_{path} \tag{1}$$

In above equation, the pump inlet, P_{Pin}, is obtained by calculating the elevation head for the cold pool sodium level and the exit pressure, P_{Po}, is the sum of the pump inlet pressure and the pump head.

The IHX flow would respond to the level difference between the two pools, as well as losses and gravity gains in the IHX. The volume-averaged momentum equations for IHX flow is:

$$\frac{dW_{1X}(k)}{dt} \sum_X \frac{L(k)}{A(k)} = P_{Xin} - P_{Xo} - \sum_X \Delta P_{f,g}(k), \qquad k = 1, \cdots, N_{path} \tag{2}$$

The IHX inlet pressure, P_{Xin}, is obtained from the static head between the hot pool level and the IHX inlet elevation and the IHX exit pressure, P_{Xo}, is the static head between the cold pool level and the IHX exit elevation. The core inlet pressure, P_{Rin}, is obtained from a complicated algebraic equation and the derivation will be discussed later.

2.1.2 Damaged System

In KALIMER, pipe rupture can only happen in the pump discharge line to the reactor. For the broken path, Eq. (1) has to be modified to:

$$\frac{dW_p}{dt} \sum_{uob} \frac{L}{A} = P_{Po} - P_{bin} - \sum_{uob} \Delta P_{f,g} \tag{3}$$

An additional equation is needed to describe the flow downsteam of the break:

$$\frac{dW_{dob}}{dt} \sum_{dob} \frac{L}{A} = P_{bo} - P_{Rin} - \sum_{dob} \Delta P_{f,g} \tag{4}$$

The inlet and outlet pressures at break locatioon, P_{bin} and P_{bo}, respectively, are calculated by break model. The external pressure for the break, P_{ext}, which is needed to compute these pressures, is obtained from the static head of the cold pool. This pressure acts as the back pressure opposing the flow out of the break. The value of this pressure is much larger than that for the loop-type design, which is generally equal to atmospheric pressure until the sodium in the guard vessel covers the break location. This will make the pipe break in the pool-type designs less sever relative to the loop-type designs.

2.2 Liquid Level in Pools

The liquid levels in the cold and hot pools can be obtained by mass balance at each pool. Total sodium mass in the cold pool is obtained by mass balance at the cold pool:

$$\frac{d}{dt}(\mathbf{r}V)_{CP} = \sum_{k=1}^{N_{path}} W_X(k) - \sum_{k=1}^{N_{path}} W_P(k) + W_{ovf} + W_b \tag{5}$$

Note that the break flow, W_b, is zero for an intact system and the overflow from the hot pool, W_{ovf}, would be zero if the hot pool level were below the top of thermal liner. Then, the cold pool level can be obtained from the sodium mass in the cold pool by assuming that the cold pool can represented by two distinct regions with the different cross-sectional area as shown in Fig. 2.

The time rate change of sodium mass in the hot pool is obtained by mass balance at the hot pool:

$$A_{HP}\frac{d}{dt}(\mathbf{r}Z)_{HP} = W_C - \sum_{k=1}^{N_{path}} W_X(k) - W_{ovf} \tag{6}$$

Eq. (6) assumes that all the level changes likely to occur during transient are confined to a constant cross-sectional area. When Eqs. (5) and (6) are solved simultaneously with the flow equations, the sodium levels for hot and cold pool during the transient can be obtained.

2.3 Reactor Internal Pressure

2.3.1 Intact system

Differentiating of the mass conservation equation at the core inlet with time yields

$$\frac{dW_C}{dt} = \sum_{k=1}^{N_{path}} \frac{dW_P(k)}{dt} \tag{7}$$

Differentiating of the mass conservation for the core can be expressed in terms of the channel flows as

$$\frac{dW_C}{dt} = \sum_{j=1}^{N_{ch}} \frac{dW_j}{dt} \tag{8}$$

where N_{ch} represents the number of channels simulated in the core. Time rate of the core flow change for each channel can be written from the momentum balance

$$\frac{dW_j}{dt}\left[\sum\frac{L}{A}\right]_j = P_{Rin} - P_{Ro} - \left[\sum \Delta P_{f,g}\right]_j \tag{9}$$

Combining Eqs. (7), (8) and (9), the core inlet pressure during the transient can be obtained.

2.3.2 Damaged System

In case of a pipe rupture in one of the pump discharge lines, mass conservation at the core inlet has to account for the downstream flow of the break to the core. Differentiating both sides with time yields

$$\frac{dW_C}{dt} = \sum_{\substack{k=1 \\ \neq brk}}^{N_{path}} \frac{dW_P(k)}{dt} + \frac{dW_{dob}}{dt} \tag{10}$$

Combining Eq. (18) with Eqs. (14) and (15) yields the core inlet pressure

2.4 Energy Balance in the Hot Pool

Thermal stratification may occur in the hot pool region if the entering is colder than the existing hot pool coolant and the flow momentum is not large enough to overcome the negative buoyancy force. Since the fluid of hot pool enters the IHXs, the temperature distribution of the hot pool can affect the overall system response. Hence, it is necessary to predict the pool coolant temperature distribution with sufficient accuracy to determine the inlet temperature conditions for the IHXs and its contribution to the net buoyancy head.

During normal reactor scram, the heat generation is reduced almost instantaneously while the coolant flow rate follows the pump coastdown. This mismatch between power and flow results in a situation where the core flow entering the hot pool is at lower temperature than the temperature of the bulk pool sodium. This temperature difference leads to the stratification when the coolant momentum is insufficient.

The stratification of the core flow in the hot pool is represented by a two-zone model. The hot pool is divided into two perfectly mixing zones determined by the maximum penetration distance of the core flow. This penetration distance is a function of the Froude number of the average core exit flow. The temperature of each zone is computed from energy balance considerations. The temperature of the upper portion, T_A, will be relatively unchanged; in the lower region, however, T_B will be changed and somewhat between the core exit temperature and the temperature of upper zone due to active mixing with core exit flow as well as heat transfer with the upper zone. The temperature of upper zone is mainly affected by interfacial heat transfer.
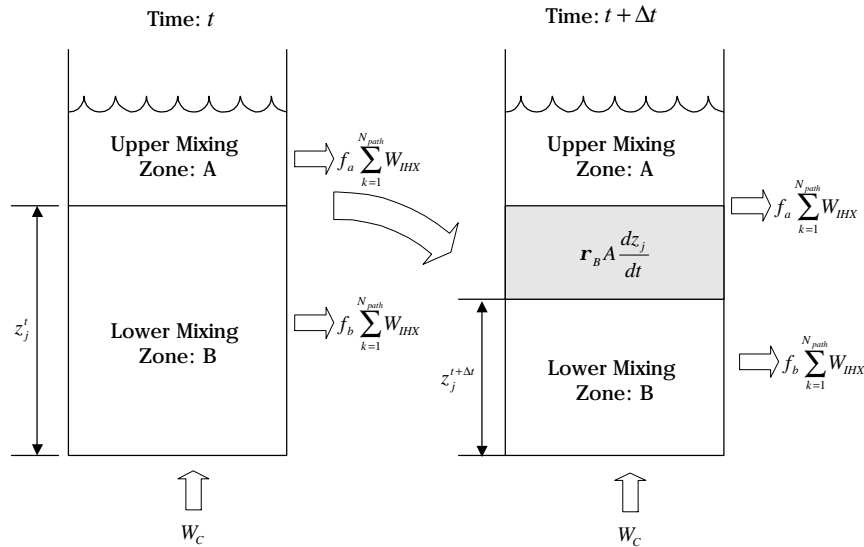

Fig. 3: Two mixing zone model for hot pool

The non-conservative form of energy balance equations which determine the various temperatures in the hot pool are given below:

2.4.1 Lower mixing zone B:
Combining energy conservation equation with mass conservation equation and rearranging the resulting equation yield the nonconservative form of energy equation:

$$\boldsymbol{r}_B V_B \frac{dE_B}{dt} = \begin{cases} \dfrac{dz_j}{dt}\,\boldsymbol{r}_A A(E_A - E_B) + W_C(E_{Ro} - E_B) - Q_{wall} - Q_{interface} & \text{if } \dfrac{dz_j}{dt} > 0 \\[2ex] W_C(E_{Ro} - E_B) - Q_{wall} - Q_{interface} & \text{if } \dfrac{dz_j}{dt} \le 0 \end{cases} \qquad (11)$$

2.4.2 Upper mixing zone A:

Combining the energy conservation equation with mass conservation equation and rearranging the resulting equation yield the nonconservative form of energy equation for upper mixing zone:

$$(\boldsymbol{r}V)_A \frac{dE_A}{dt} = \begin{cases} -Q_{wall} - Q_{cgas} + Q_{interface} & \text{if } \dfrac{dz_j}{dt} > 0 \\[2ex] \dfrac{dz_j}{dt}\,\boldsymbol{r}_B A(E_B - E_A) - Q_{wall} - Q_{cgas} + Q_{interface} & \text{if } \dfrac{dz_j}{dt} \le 0 \end{cases} \qquad (12)$$

2.5 Energy Balance in the Cold Pool

Currently, perfect mixing of the IHX flow with the cold pool sodium is assumed. Energy balance equation for the cold pool is derived as:

$$(\boldsymbol{r}V)_{cp} \frac{dh_{cp}}{dt} = \sum_{N_{path}} W_{IHX} h_{IHX} - h_{cp} \sum_{N_{path}} W_{IHX}$$
$$+ W_{ovf} h_{hp} - W_{ovf} h_{cp} + \sum_{N_{path}} W_{brk} h_{brk} - h_{cp} \sum_{N_{path}} W_{brk} \qquad (13)$$

2.6 Nuclear Plant Analyzer (NPA)

The conventional method to handle the code outputs is not inconvenient to analyze the simulation results. The main reason for this inconvenience is that the use of text-oriented
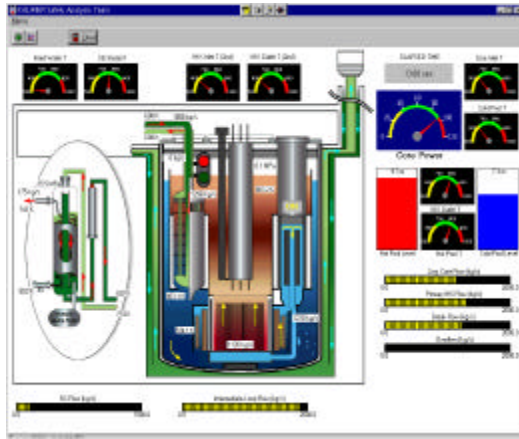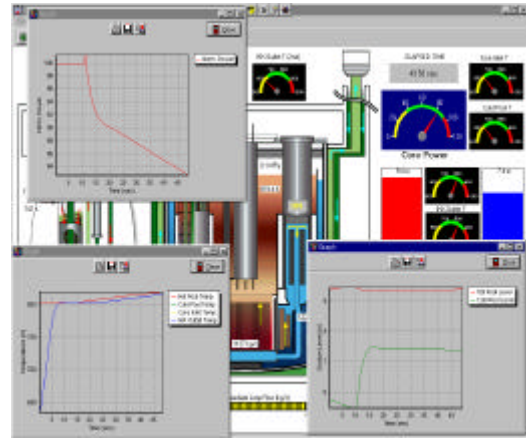

Fig. 4: Plant mimic

Fig. 5: X-Y graphs in KALIMER NPA

programming. The plant analyzer using graphical user interface makes it possible to analyze the simulation results while the code is executing. The code can be executed within NPA environment and all the key parameters are shown in either text or graphical forms. The user dialog box to select the

variables for X-Y graphs is provided and the coordinates for selected graphs are modified dynamically with simulation time. The some of features of the KALIMER NPA are shown in Figs. 4 and 5.

3. RESULTS

The modeling described here was implemented in the SSC-K code and then tested on the problem representing unscrammed loss of heat sink (ULOHS) accident with pump dischage pipe break to investigate if the models are working as intended. The nominal operating condition for KALIMER was selected as an initial condition for the test problem [3]. The transient was initiated by assuming the secondary loop heat transfer is arbitrarily terminated at 0.0 s and followed by the pump discharge pipe break at 10 s. The EM pumps continue to operate normally, and plant protection system is assumed not to scram the reactor. The passive decay heat removal system is not modeled for this transient. The transient was terminated after 2000 s.
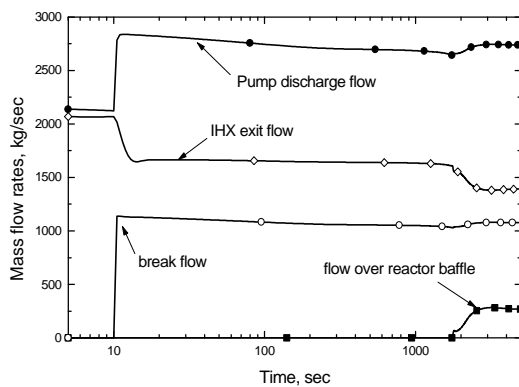

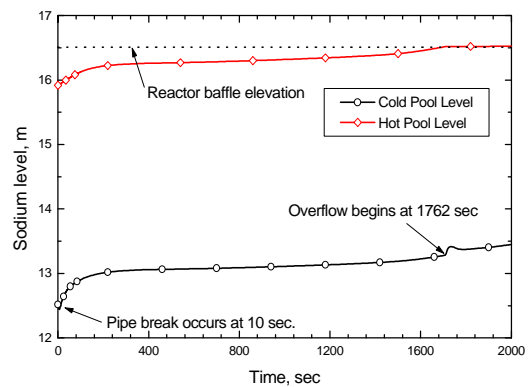Fig. 6: Mass flow rates for primary system
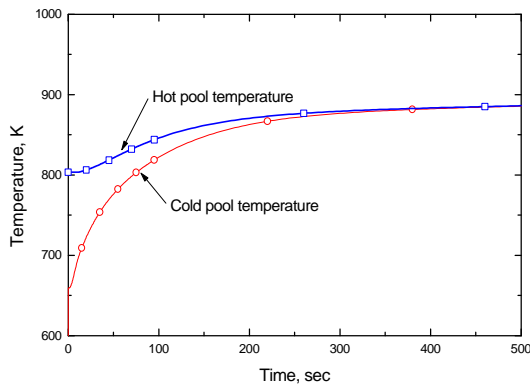

Fig. 7: Hot and cool pool sodium levels

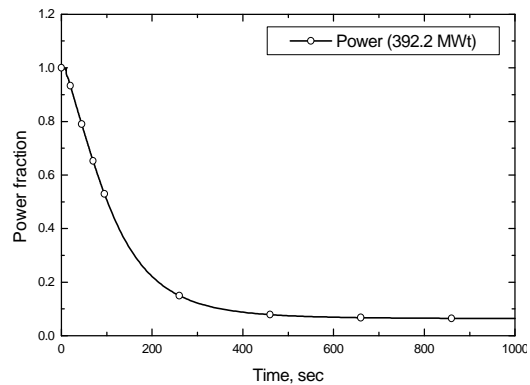Fig. 8: Hot and cool pool sodium temperatures

Fig. 9: Normalized core power

Fig. 6 shows the various mass flow rates in the primary system. When the pipe break occurs, the break flow increases upto a certain value and decreases slowly due to sodium density decrease. The pump discharge flow also increases because overall pressure drop becames smaller. However, the primary side of the IHX flow decreases as core inlet flow decreases. At ~1800 s, the sodium level of the hot pool becames higher than the divider elevation and the sodium above reactor baffle is flooded into the cold pool. The sodium levels for the hot and cold pools are shown in Fig. 7. The cold pool sodium level increases rapidly as break flow is initiated. The slow increase of the hot and cold pool sodium levels is due to the average sodium temperature increase (Fig. 8). When the hot pool sodium

level reaches the core baffle elevation, the overflow to the cold pool is initiated. Fig. 8 shows the average hot and cold pool temperatures. The temperature increase of the cold pool sodium is delayed because of the large sodium inventory. At ~300 s, the cold pool sodium temperature becomes identical with the hot pool sodium temperature. As can be seen in Fig. 9, the reactor power drops to decay heat level by ~400 s due to negative reactivities. The increase in sodium temperature results in the all feedback reactivities except sodium density reactivity to negative values.

5. CONCLUSIONS

The modeling devloped for KALIMER transient analysis has been tested with the unscrammed loss of heat sink (ULOHS) accident with pump dischage pipe break. The priliminary test results show that the models implemented in SSC-K work properly in qualitative sense. However, the code validation   has to be made in order to use in KALIMER design application.

Acknowledgements

REFERENCES

[1] H. C. Kim et al., "Kalimer Design Concept Report," KAERI/TR-888/97.

[2] A. K. Agrawal et al., "An Advanced Thermohydraulic Simulation Code for Transients in LMFBRs (SSC-L Code)," BNL-NUREG-50773, Brookhaven National Laboratory, 1973.

[3] Y. M. Kwon et al., "SSC-K Basedeck for KALIMER Safety Analysis," KALIMER-SA-CA001, Rev. 0, 1998.